Chemical Engineering Journal 158 (2010) 32–38

Contents lists available at ScienceDirect

Chemical Engineering Journal

journal homepage: www.elsevier.com/locate/cej

Complementary imaging of oil recovery mechanisms in fractured reservoirs

G. Ersland [a,*], M.A. Fernø [a], A. Graue [a], B.A. Baldwin [b], J. Stevens [c]

[a] University of Bergen, Norway
[b] Green Country Petrophysics LLC, OK, USA
[c] ConocoPhillips, OK, USA

ARTICLE INFO

Article history:
Received 5 May 2008
Received in revised form
25 November 2008
Accepted 26 November 2008

Keywords:
Enhanced oil recovery
Wettability
MRI
NTI
Fractured reservoirs

ABSTRACT

Complementary imaging techniques used to study enhanced oil recovery (EOR) processes in fractured oil reservoirs have provided new and improved fundamental understanding of how oil recovery is affected by fractures. The combination of two imaging techniques such as magnetic resonance imaging (MRI) and nuclear tracer imaging (NTI) enables a complementary investigation on materials and processes, where large scale (~m) phenomena are controlled by small scale (μm) heterogeneities. MRI provides high spatial resolution and fast data acquisition necessary to capture the processes that occur inside fractures less than 1 mm wide, while NTI provides information on macro-scale saturation distribution in larger fractured systems. The oil recovery mechanisms involved with waterflooding fractured chalk blocks were found to be dependent on the wettability of the chalk, as the wettability had great impact on the fracture/matrix hydrocarbon exchange. The MRI images of oil saturation development inside the fractures clearly revealed two distinct transport mechanisms for the wetting phase across the fracture at several wettability conditions, and provided new and detailed information on fluid fracture crossing previously observed in block scale experiments investigated by NTI. The ability to obtain rapid (~s) 1D saturation profiles, high spatial resolution 2D images (sagital, transverse and coronal) within minutes and detailed 3D images within a couple of hours, makes MRI a powerful tool in studies of multiphase flow in fractured porous rocks, and provides excellent dynamic information of enhanced oil recovery efforts.

1. Introduction

The low permeability chalk reservoirs in the southern part of the North Sea are distinguished by intense fracturing that occurs due to tectonic activity. As a result, the oil reserves in these reservoirs, found in the abundant porosity in the chalk matrix, are located in distinct blocks surrounded by interconnected or isolated open, or partly open, fractures. Production of oil from fractured reservoirs is generally believed to be governed by spontaneous imbibition of water from the fracture network into the matrix, and the subsequent movement of the expelled oil through the same fracture network and towards the production wells. Great efforts have been made to map these processes to obtain a fundamental understanding of the mechanism involved and, in turn, achieve new insight to strategies for enhanced oil recovery (EOR). The recovery efficiency in fractured chalk reservoirs using standard production methods is significantly lower compared to sandstone reservoirs. The potential EOR target is accordingly higher.

The applications of magnetic resonance imaging (MRI) for characterizing core samples and flow properties of porous materials are known and a considerable amount of literature has been published on the topic. Previous articles have discussed MRI imaging for core characterization purposes [1,2], the monitoring of imbibition and displacement processes [1,3] and the application of MRI to the study of formation damage [4,5]. Recent studies have reported flow behavior and production mechanisms in fractured chalk and their dependency of wettability [6–8], rate and fracture aperture [7], and fracture configurations [8].

Nuclear tracer imaging (NTI) of fluid flow in fractured larger block sized models of chalk ($L \times W \times H = 20\,\text{cm} \times 5\,\text{cm} \times 10\,\text{cm}$) has been studied since the mid 1990s [9–13]. Much of this work has been devoted to the wettability effects on *in situ* fluid saturations and oil recovery mechanisms. In addition, the effect of fracture permeability on flow behavior has been reported using the same technique [14]. The NTI method enables fluid saturation information in larger porous rock sample systems than the MRI, but at the cost of less spatial and temporal resolution.

The intent of this paper is to summarize the results and the relevance of the NTI- and MRI flow visualization techniques, and describe our efforts to develop procedures for validating NTI results from larger fractured blocks using MRI on smaller core samples

* Corresponding author at: University of Bergen, Department of Physics and Technology, Allègaten 55, 5011 Bergen, Norway. Tel.: +47 55582868; fax: +47 55589440.
E-mail address: geir.ersland@ift.uib.no (G. Ersland).

1385-8947/$ – see front matter © 2008 Elsevier B.V. All rights reserved.
doi:10.1016/j.cej.2008.11.049

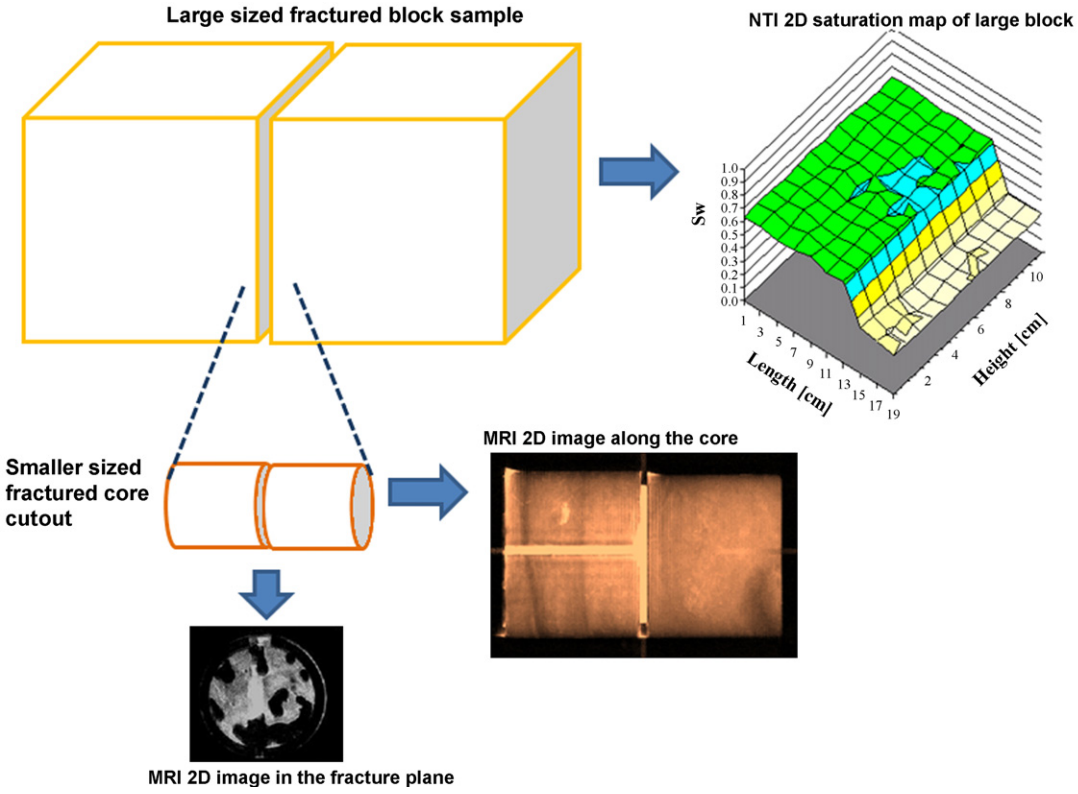

Fig. 1. Complementary imaging of fractured porous media using NTI and MRI.

(Fig. 1). This paper focuses on results and technical knowledge gained on chalk models the last 10 years and attains to describe issues related to imaging in more detail.

2. Nuclear tracer imaging

The NTI method measures the intensity of γ-radiation from isotopes dissolved in one or more of the fluids present and is a further development from the technique described by Baily et al. [15]. For imaging fluids in porous rocks, the choice of radioactive tracers should be determined following consideration of predominantly three aspects: (1) high energy to penetrate rock samples and pressure chamber, (2) sufficiently long half-life to minimize correction due to natural decay, and (3) the tracer should be soluble in only one of the fluid phases. Generally, in a system where n phases are to be identified, $n-1$ tracers are needed. Thus, during oil–water displacements, when only oil and water is present in the pore space, one tracer is sufficient to image the fluid development since the fractional water saturation, S_w, and fractional oil saturation, S_o, always adds up to one and related as $S_w = 1 - S_o$. Based on this, a radioactive sodium isotope (^{22}Na) is found to be best suited water phase tracer, especially since sodium is already naturally present in the brine solution. In tests where the oil phase is imaged explicitly, such as a three phase tests, the radioisotope ^{59}Fe is added to the oil phase, which does not mix with the water. In a multi-tracer experiment, two or more radioisotopes are used simultaneously and the various γ-tracers are identified by their characteristic γ-emitting energies. Therefore, a detection system with high energy resolution is required, preferentially in the order of 2 keV at FMHW (full maxima at half width). Isotopes used in recent studies are listed in Table 1.

One of the advantages of using nuclear tracers is its impassive nature with respect to the delicate network of pores when possible salt absorption is minimized by preflushing with regular brine. The possibility to perform multiple experiments on the same rock sample allows for experimental reproduction and investigation of impacts on flow- and recovery mechanisms from a single parameter (e.g. rate, wettability or fracture). Also, the NTI technique has the capability of imaging the 1D *in situ* oil production in cores up to 2 m in length, thus minimizing the disturbance from capillary end-effects, and enabling large scale gravity drainage experiments with local saturation measurements. Obvious disadvantages are the radioactivity, the low temporal and spatial resolution and the laboratory space required to accommodate rigs and instruments. However, experience has shown that larger scale fluid displacement experiments have great benefits, and the displacement rate is generally well within the reservoir analogue.

2.1. Fluid saturation calculations

Radioactivity is a spontaneous nuclear phenomenon insensitive to temperature and pressure with statistical uncertainty given by $\Delta d = 1/\sqrt{d}$, thus, uncertainty will decrease with increased counting time and tracer concentration. The counting time needed to obtain a sufficiently low uncertainty is greatly reduced when using higher tracer concentrations. A compromise between tracer concentration and counting time was found based on the aim of each experiment. If the main objective is to capture the local change in fluid saturation as a function of time, the counting time and number of points along the core should be hold to a minimum. However, if the objective is to capture local heterogeneity in porosity, the counting time should be

Table 1
Properties of commonly used isotopes.

Isotope	Half-life	Energy γ_1 (keV)	Energy γ_2 (keV)	Labeled phase
^{22}Na	2.6 years	511	1275	Water
^{60}Co	5.3 years	1173	1333	Water
^{59}Fe	45 days	1099	1292	Oil

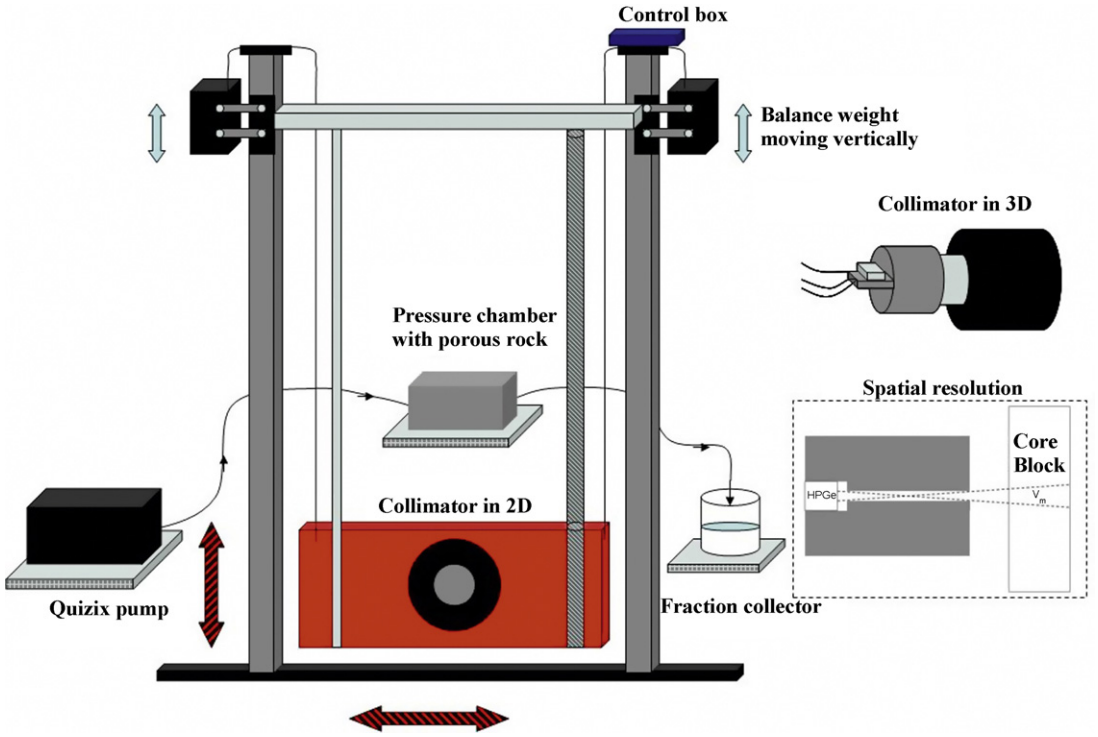

Fig. 2. Schematic of vertical flow rig.

large to minimize uncertainty. Typical NTI experiments have tracer concentrations of about 1–2 mCi/L (1 mCi = 37 MBq), with a corresponding counting time of about 3 min at each position along the core. This gives a total counting time of 6–7 h per image, which would generate a total of 10–15 images of the entire displacement process. Uncertainties for an arbitrary point of saturation with these settings will generally be in the range of 3–5%. The average saturation from NTI generally matches the material balance within 3–4%. The NTI 2D saturation images do not capture the saturation development inside the fracture(s), and do not, in a strict sense, represent a snapshot of the saturation distribution, as the saturation will change while imaging. However, the saturation change is slow, usually within a few percent per image, and generally of minor significant when interpreting the image series.

The water saturations are found from the linear relationship between the number of disintegrations and the saturation of the labeled fluid by

$$S_w = \frac{d - B}{d_{100\%} - B} \quad (1)$$

where S_w is the water saturation in fraction of pore volume, d is the number of disintegrations recorded (radiation intensity) at a given point and B is the number of background counts without the tracer present. $d_{100\%}$ represents the radiation intensity when the core is fully saturated with radioactive brine. For a block experiment, the radiation intensity at $S_w = 100\%$ is a measure of the local porosity variations and generates a 2D porosity field plot of the whole rock sample. This intensity image is used to normalize the relative change in radiation intensity during a waterflood to calculate fluid saturations.

Nuclear tracer technology is useful in dispersion analysis by measuring the effluent production with respect to radiation intensity. For single phase flow, the effluent profile in a brine-radioactive brine displacement provides useful information about the pore topology, i.e. heterogeneity and dead-end pore fractions. In fractured reservoirs, tracer tests are commonly used to describe petrophysical properties of the fracture network from injector to producer. Laboratory dispersion studies of large scale fractured core blocks using tracer technology is an option to determine dispersion coefficients in fracture network, and could benefit the interpretation of field scale tracer tests.

Another application for NTI is studies of connate water and injection water mixing. This is carried out with two water soluble tracers, e.g. Na^{22} and Co^{60}, one tracer labeling the connate water and the other the injection water. Laboratory tests with two tracers have been used to predict deep penetration of injection water into chalk formations saturated with oil and connate water [16].

2.2. Flow rigs and instrumentation

A horizontal porous 1D rig capable of scanning 1.5 m long core samples, and a vertical 2D rig for imaging large scale blocks have been used to study large scale displacement processes. The vertical rig (Fig. 2) allows for simultaneous investigations of the impacts from gravity-, capillary- and viscous forces. The radiation intensity is recorded by a germanium detector and stored using a Canberra multi-channel analyzer (MCA), before the spectra are electronically processed to obtain the fluid saturation information. The detector is collimated with lead that effectively reduces the background radiation and increase the resolution of the system.

2.3. NTI of waterfloods in chalk blocks with different wettabilities

Previous NTI work reports that oil recovery mechanisms change significantly with the wettability condition of isolated matrix blocks of fractured chalk rock samples [11–13,17]. At strongly water-wet conditions, the dominating mechanism was spontaneous imbibition of water from fracture to matrix, displacing oil from each isolated matrix block until the endpoint for spontaneous imbibition was reached. At this point, the matrix capillary pressure is zero, and equal to the capillary pressure in the fracture. At moderately water-wet conditions, the presence of fractures was less

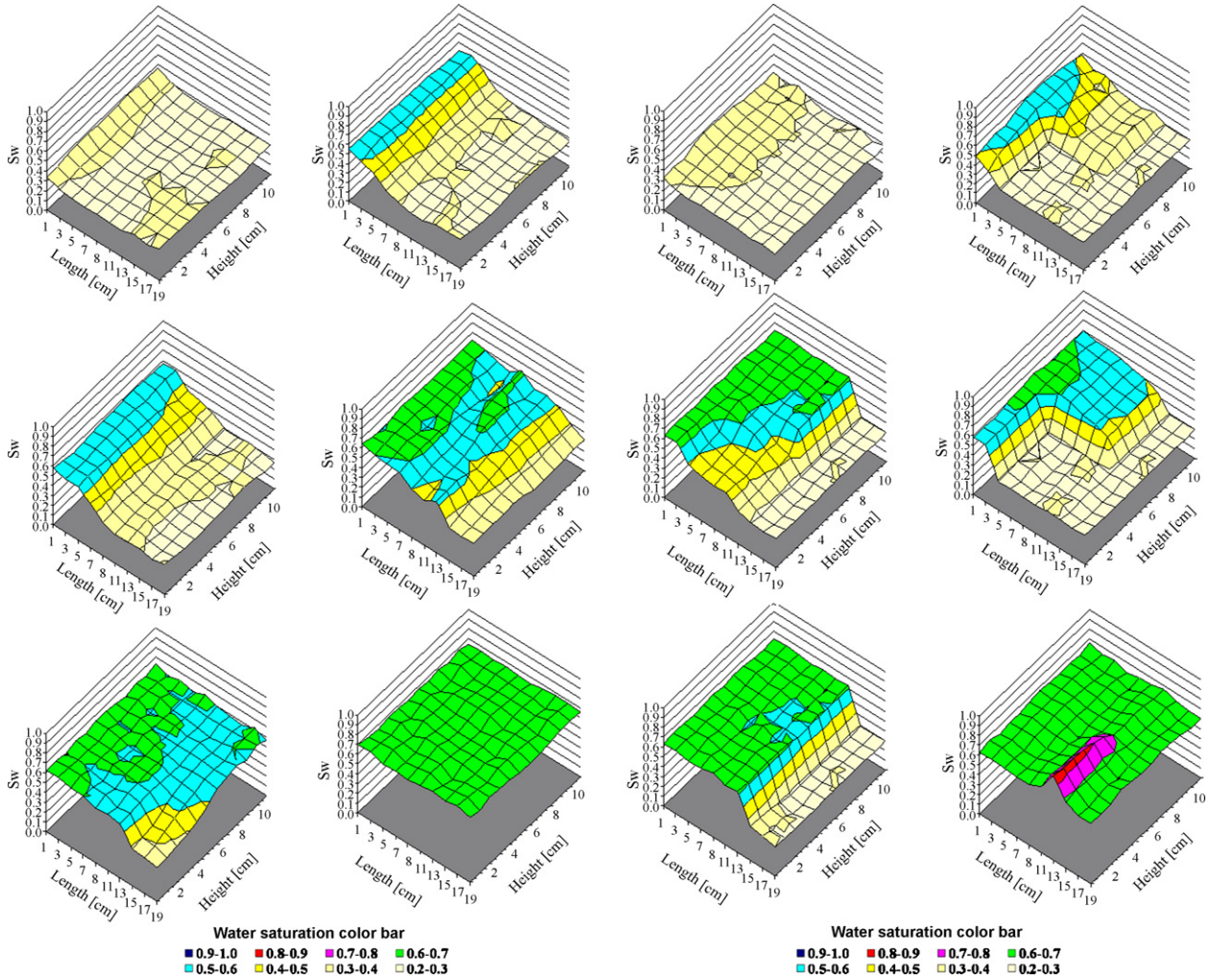

Fig. 3. NTI of waterflood in fractured chalk blocks. The strongly water-wet case is shown in the two left columns, and the moderately water-wet case in the two right columns.

prominent and water displaced oil with a uniform dispersed front. Water swept across fractures, through capillary contacts, increasing the total oil recovery by adding a viscous component to the displacement. Fig. 3 demonstrates the effect of wettability, and compares the *in situ* water saturation development at various pore volumes (PV) injected during waterfloods at strongly water-wet wettability conditions (left) to moderately water-wet (right) in fractured chalk blocks. The embedded fracture network was identical for each waterflood and is shown in Fig. 4.

The wettability of initially strongly water-wet outcrop rock samples was altered by aging in stock tank crude oil at elevated temperature for a selected period of time as described in [17]. A range of wettabilities from strongly water-wet to near-neutral wet was created in the laboratory by varying the time the crude oil was exposed to the rock surface. Moderately water-wet conditions reflect in this case an Amott-Harvey water index, I_w, of 0.6. As can be seen from Fig. 3, the waterfront propagation for the moderately water-wet block is much more uniform compared to the block by block displacement for the strongly water-wet case. This observation indicates that the recovery mechanisms change towards more viscous dominant flow regimes at less water-wet conditions.

In summary, monitoring fluid flow with nuclear tracer imaging in fractured blocks of chalk gives quantitative and qualitative information of how the recovery mechanisms are affected by fractures. The water saturation in individual matrix blocks was measured as function of time, and the role of horizontal capillary continuity contributing to oil recovery through a viscous pressure component in waterfloods was determined for different wetting states. However, the NTI technique failed to image the detailed wetting phase transport mechanism(s) inside fractures. Important questions that arose were how capillary continuity was established, and how this contact contributed to increased oil recovery. These questions articulated the motivation behind increasing the spatial imaging resolution by using MRI tomography on smaller samples.

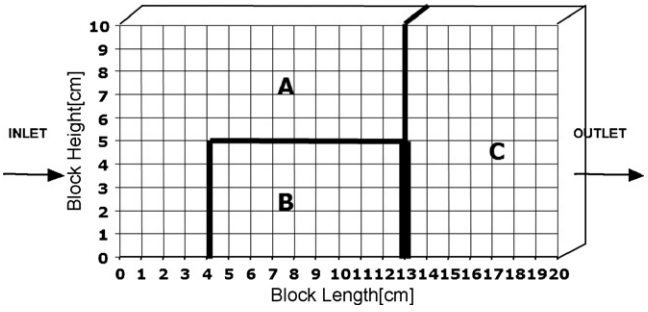

Fig. 4. Fracture configuration.

3. Magnetic resonance imaging

The MRI instrument (Unity/Inova-Imaging 85/310 spectrometer, Varian Inc., Palo Alto, CA) used is a proton imager located in the ConocoPhillips Technology Center in Bartlesville, Oklahoma, USA.

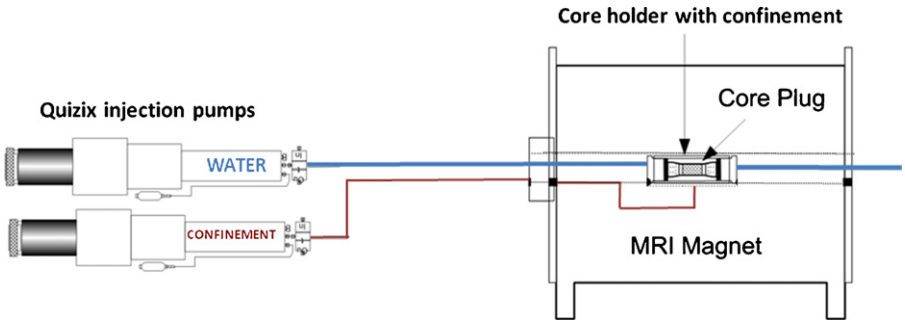

Fig. 5. Schematic of MRI experiments.

The super conductive magnet induces a static magnetic field with strength 2 T, and operates at a resonance frequency for hydrogen at 85.7098 MHz. In order to obtain fast saturation information we use quantitative one-dimensional specific profiling along with fast two-dimensional imaging in displacement experiments with stacked core plugs. High quality fluid saturation profiles (signal-to-noise ratio > 30) were generally acquired within 20–30 s. Images of two-dimensional slices, with slice thickness from 1 to 30 mm, either within the fracture plane (transverse image (y–z-plane)) or aligned parallel with the flow direction (sagital (x–y-plane) or coronal image (x–z-plane)) were acquired within 8 min, with four averages. A full 3D image of the core system was performed to capture the complete fluid saturation distribution, and required from 2 to 9 h to complete, depending on signal-to-noise ratio. The use of 3D during displacement tests was limited due to the fast imaging required during flooding experiments. To distinguish between the two liquid phases, water and oil, the regular brine was exchanged with D_2O brine. D_2O is insensitive to magnetic resonance and reveals no signal above the background level (detected as black dots on the MRI images). To ensure efficient brine replacement, the remaining H_2O-brine in the core sample was measured by NMR spectroscopy (MARAN low field spectrometer). Generally, for relatively low displacement rates, the residual H_2O was below 2%PV.

The MRI system consisted of the core sample, a core holder to maintain overburden pressure, and the MRI to monitor the distribution of water and oil (Fig. 5). Fluorinert (FC-40) was used as the confinement fluid. Fluorinert is a fluorocarbon and contains no hydrogen atoms, thus it is not imaged, and its low dielectric properties minimize RF losses. The core holder was made of composite material making it transparent to the RF pulses in the MRI. The confinement pressure and water injection rates are controlled by Quizix pumps, or water column for low constant pressure experiments. In recent experiments, however, the core plugs have been confined using epoxy coating. This approach has been quit successful for low pressure displacement processes. The epoxy has proven to hold pressures up to 8 bars, and allows for pressure measurement inside the fracture by inserting pressure ports through the epoxy rim.

3.1. Fluid saturation calculations

The MRI experiments were performed without removing the cell from the MRI apparatus when initiated. With oil being the only fluid present that contributes to MRI intensity after regular brine was replaced with a saline D_2O, the image intensity represents the oil phase. The main objective for these experiments was to provide qualitative dynamic information of the fluid transfer between matrix blocks and fractures. In addition, quantitative spatial information of fluid saturations in larger regions of interest in chalk where obtained by the following relation:

$$S_o = S_{o,i}\frac{I - B}{I_i - B} \tag{2}$$

where $S_{o,i}$ is the initial saturation of oil, I is the average MRI signal intensity at a given time during the displacement, B is the background noise and I_i is the initial MRI signal intensity. A linear relationship between the average MRI Intensity and remaining oil saturation was found experimentally when averaging over the whole core. The chalk material was favorable for MRI imaging due to a uniform and sharp distribution of pores and low magnetic disturbance in minerals. The MRI intensity was not perfectly linear over the entire saturation range, but a good linear relationship was found between irreducible water saturation and residual oil saturation. All the images were acquired with standard spin-echo sequences. The echo time was generally from 3 to 5 ms and the repetition time was around 1 s. The T_2 relaxation time for a fully oil-saturated core plug was 1074 ms.

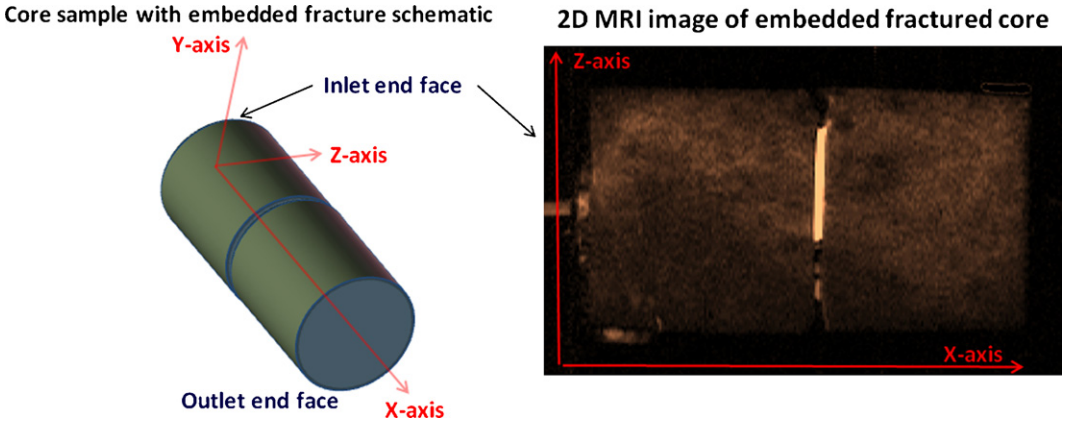

Fig. 6. Slice selection in the X–Z plane. Matrix (Grey) and fracture (white line).

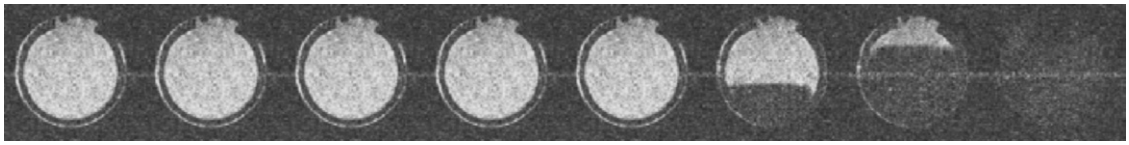

Fig. 7. Development in water saturation inside the transverse fracture (*Y–Z* plane) at water-wet conditions. Water starts to fill fracture from the bottom (third image from the right).

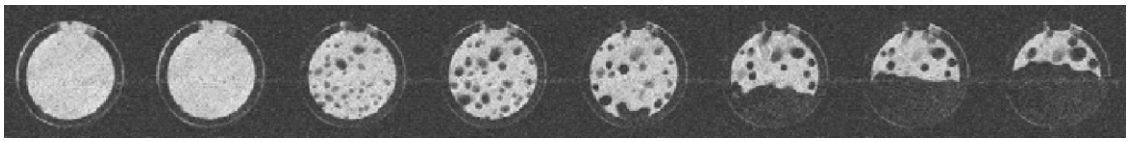

Fig. 8. Development in water saturation inside the transverse fracture (*Y–Z* plane) at moderately water-wet conditions. Water liquid bridges accelerate fluid transport across fracture (third image from the left).

3.2. Imaging flow within fractures

Fractures can easily be identified as these initially are filled with either oil or D_2O. The latter can be identified as an area with low signals, while the former appears as an intense narrow band. Fig. 6 shows the slice selection for a recent experiment covering both oil filled fractures and the three individual matrix blocks. A schematic of the fractured core is included to illustrate imaging orientation and clarify the imaging. The images were acquired automatically by running each slice series in sequence. Data was collected with 512 by 256 points for read-out. Field of view was set to 60 mm × 60 mm for the transverse image and 110 × 60 for sagital and coronal images. The images are imported as floating point files either in MS Excel or MatLab. Regional saturations are found from the linear relationship between MRI intensity and oil saturation.

As discussed in Graue et al. [6] and Aspenes et al. [7], the MRI images of water saturation development in the fracture clearly revealed two distinct mechanisms for wetting phase transport in a stacked system with an open embedded fracture of 2–3 mm aperture (see Figs. 7 and 8). When strongly water-wet, the inlet plug reached its spontaneous imbibition endpoint (zero capillary pressure) before water entered the fracture. The water filled the fracture from the bottom and displaced the oil upwards at the rate of water injection. The water is detected as no signal (black) whereas the oil appears bright on the MRI images (see Fig. 7).

The very same experiment was performed at less water-wet conditions (Fig. 8). At this wettability, water droplets formed on the exit face of the inlet plug and grew large enough to form individual bridges between the two plugs. This occurred well before the inlet plug reached its spontaneous imbibition endpoint. Under these conditions, the fracture filled slowly with water when the bridges increased in diameter and additional ones formed uniformly distributed across the cross-sectional fracture plane. A viscous pressure drop was established across the stacked core plugs due to the capillary continuity of the wetting phase, providing a viscous component to the total oil recovery. This observation corroborated earlier larger scale NTI experimental results on the effect of fractures during waterflooding at highly water-wet and moderately water-wet conditions [10].

3.3. Introducing an escape fracture

In the stacked core system with one open fracture perpendicular to the flow direction, as shown in Figs. 7 and 8, water will ultimately forced to enter the downstream outlet core plug due to limited alternative exits and a constant supply of water at the inlet end face. To confirm whether or not water phase capillary continuity in the form of water bridges would be established with alternative outlets, the outlet core was cut in two along the flow direction to create an escape fracture (see Fig. 9).

The results from this study [8] showed that wetting phase bridges across open fractures formed despite having alternative outlets with higher flow properties (the escape fracture). The study also showed that the bridges added a viscous component to recovery of oil from the blocks surrounded by fractures. Water bridges were stable for days and resulted in oil recovery far exceeding the spontaneous imbibition potential.

Fig. 10 shows MRI images of water forming bridges (black dots) on the exit face of each isolated core halves (bright semicircles on images), rather than escaping through the outlet fracture. The

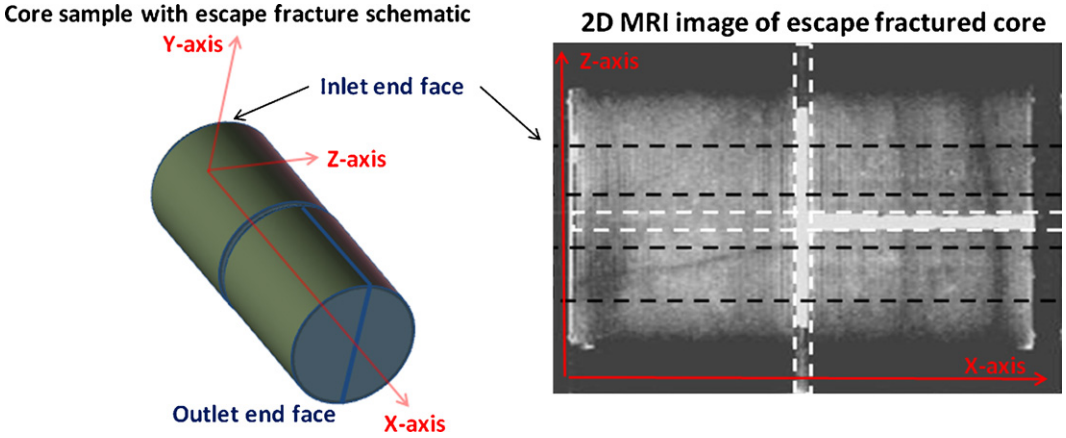

Fig. 9. Slice selection in the *X–Z* plane during the escape fracture tests. Matrix (black dots) and fractures (white dots).

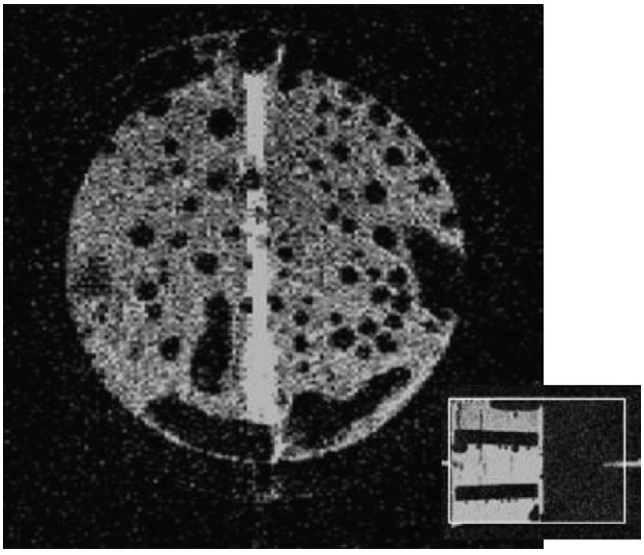

Fig. 10. Fracture crossing in the escape fracture setup. MRI images show oil and water distribution in the transverse (*Y–Z* plane) fracture, and in the escape fracture (*Y–X* plane, inserted image) during the waterflood. Water (D_2O) appears as the black phase.

results were similar during constant injection pressure (1 psi/foot) than during constant injection rate (with a maximum pressure of 10 psi/foot), although fewer bridges was formed due to higher water flux across the fracture. In both experiments, the water saturation obtained from MRI intensities in the isolated blocks was approximately 53%. For comparison the spontaneous imbibition end point was $S_w = 38\%$. Hence, the viscous component exerted by wetting phase bridges across open fractures added significantly to the total oil recovery. However, the oil recoveries from isolated blocks are not further increased by increasing the differential pressure above 1 psi/foot. This result shows that the increased oil recovery is due to the increased pressure differential across the isolated matrix blocks exerted by the water bridges. At the same time there seems to exist a maximum pressure, or viscous component, that the bridges may transfer across the fracture, since the recovery of oil did not increase further with a 10-fold pressure increase during the constant flow experiment. The added pressure will exceed what the water bridges are able to exert on the adjacent matrix blocks and no further oil will be recovered.

4. Conclusions

- Nuclear tracer imaging provided information on macro-scale saturation distribution development that result from the fractures in porous rock models.
- Magnetic resonance imaging provided high spatial resolution imaging and fast data acquisition necessary to capture the processes that occur inside fractures 1 mm wide.
- Small scale MRI results corroborated larger scale NTI results where the influence of wettability during waterflooding in fractured rock samples at strongly water-wet and moderately water-wet wettability conditions was studied.
- Complimentary imaging provided detailed explanation of fluid flow mechanisms important in enhanced oil recovery.
- MRI tomography provided fast and high quality fluid saturations information and showed a significantly higher recovery than the normally assumed spontaneous imbibition end point in isolated matrix blocks.
- Viscous recovery provided by water bridges across open fractures may explain the oil recovery mechanisms in chalk reservoirs in the North Sea.

References

[1] B.A. Baldwin, R. King, Why would an oil company use MRI, in: P. Blumler, B. Blumich, R. Botto, E. Fukushima (Eds.), Spatially Resolved Magnetic Resonance (Methods, Materials, Medicine, Biology, Rheology, Geology, Ecology, Hard Wave), Wiley-VCH, New York, 1999.
[2] A.E. Lothe, R.H. Gabrielsen, N. Bjørnevoll Hagen, B.T. Larsen, An experimental study of the texture of deformation bands: effects on the porosity and the permeability of sandstones, Petroleum Geoscience 8 (2002) 195–207.
[3] S. Chen, F. Qin, K. Kim, A. Watson, NMR imaging of multiphase flow in porous media, AIChE Journal 39 (6) (1993) 925–934.
[4] E. Fordham, T. Roberts, T. Carpenter, L. Hall, C. Hall, Dynamic NMR imaging of rapid depth filtration of clay in porous media, AIChE Journal (1991) 1900–1903.
[5] C. Zwagg, F. Stallmach, J. Hanssen, Applications of NMR and CT-analytical methods to assess the formation damage potential of drilling fluids, in: Int. Sym. of SCA, Proc., SCA 9813, 1998, pp. 1–12.
[6] A. Graue, E. Aspenes, R.W. Moe, B.A. Baldwin, A. Moradi, J. Stevens, D.P. Tobola, MRI tomography of saturation development in fractures during waterfloods at various wettability conditions, in: SPE 71506, Proc. SPE ATCE, New Orleans, Louisiana, 2001.
[7] E. Aspenes, A. Graue, B.A. Baldwin, A. Moradi, J. Stevens, D.P. Tobola, Fluid flow in fractures visualized by MRI during waterfloods at various wettability conditions—emphasis on fracture width and flow rate, in: SPE 77338, Proc.: SPE ATCE, San Antonio, Texas, 2002.
[8] E. Aspenes, Wettability effects on oil recovery mechanisms in fractured chalk, Dr. Scient Thesis, UoB, https://bora.uib.no/bitstream/1956/2064/7/Main+Thesis_Aspenes.pdf, 2006.
[9] B.G. Viksund, A. Graue, B. Baldwin, E. Spinler, 2-D imaging of waterflooding a fractured block of outcrop chalk, in: Proc.: 5th Chalk Research Symposium, Reims, France, 1996.
[10] B.G. Viksund, T. Eilertsen, A. Graue, B. Baldwin, E. Spinler, 2D-Imaging of the effects from fractures on oil recovery in larger blocks of chalk, in: Reviewed Proc, International Symposium of the Society of Core Analysts, Calgary, 1997.
[11] A. Graue, B.G. Viksund, B.A. Baldwin, E. Spinler, Large scale imaging of impacts of wettability on oil recovery in fractured chalk, SPE Journal 4 (1997).
[12] A. Graue, R.W. Moe, B.A. Baldwin, Comparison of numerical simulations and laboratory waterfloods with in-situ saturation imaging of fractured blocks of reservoir rocks at different wettabilities, in: SPE59039, SPE Internatl. Petr. Conf. and Exh., Villahermosa, Mexico, 2000.
[13] A. Graue, T. Bognø, B.A. Baldwin, E.A. Spinler, Wettability effects on oil recovery mechanisms in fractured reservoirs, in: SPE74335, SPEREE, vol. 4, no. 6, 2001, pp. 455–466.
[14] A. Graue, K. Nesse, Impact of fracture permeability on oil recovery in moderately water-wet fractured chalk reservoirs, in: Proc.: SPE/DOE 13th Sym. on IOR, Tulsa, Oklahoma, 2002.
[15] N.A. Baily, P.R. Rowland, D.P. Robinson, Nuclear measurements of fluid saturation in EOR flood experiments, in: Proc., European Symposium on EOR, Bornmouth, England, 1981.
[16] U. Korsbech, H.K. Aage, B.L. Andersen, K. Hedegaard, N. Springer, Measuring and modeling the displacement of connate water in chalk core plugs during water injection, SPE Reservoir Evaluation & Engineering Journal 9 (3) (2006).
[17] A. Graue, B.G. Viksund, B.A. Baldwin, Reproducible wettability alteration of low-permeable outcrop chalk, in: SPE Res. Eng. and Evaluation, April ed., 1999.